# Grating-patterned FeCo coated surface acoustic wave device for sensing magnetic field

Wen Wang, Yana Jia, Xufeng Xue, Yong Liang, and Zhaofu Du

Citation: AIP Advances **8**, 015134 (2018); doi: 10.1063/1.5012579
View online: https://doi.org/10.1063/1.5012579
View Table of Contents: http://aip.scitation.org/toc/adv/8/1
Published by the American Institute of Physics

# Grating-patterned FeCo coated surface acoustic wave device for sensing magnetic field

Wen Wang,[1,a] Yana Jia,[1,2] Xufeng Xue,[1] Yong Liang,[1] and Zhaofu Du[3]
[1]*Institute of Acoustics, Chinese Academy of Sciences, Beijing 100190, China*
[2]*University of Chinese Academy of Sciences, Beijing 100049, China*
[3]*Research Institute of Foundational Materials, Central Iron and Steel Research Institute, Beijing 100081, China*

(Received 7 November 2017; accepted 15 January 2018; published online 31 January 2018)

This study addresses the theoretical and experimental investigations of grating-patterned magnetostrictive FeCo coated surface acoustic wave (SAW) device for sensing magnetic field. The proposed sensor is composed of a configuration of differential dual-delay-line oscillators, and a magnetostrictive FeCo grating array deposited along the SAW propagation path of the sensing device, which suppresses effectively the hysteresis effect by releasing the internal binding force in FeCo. The magnetostrictive strain and ΔE effect from the FeCo coating modulates the SAW propagation characteristic, and the corresponding shift in differential oscillation frequency was utilized to evaluate the measurant. A theoretical model is performed to investigate the wave propagation in layered structure of FeCo/$LiNbO_3$ in the effect of magnetostrictive, and allowing determining the optimal structure. The experimental results indicate that higher sensitivity, excellent linearity, and lower hysteresis error over the typical FeCo thin-film coated sensor were achieved from the grating-patterned FeCo coated sensor successfully.  https://doi.org/10.1063/1.5012579

## I. INTRODUCTION

Recently the surface acoustic wave (SAW) sensors employing magnetostrictive thin film as sensitive interface supply a new approach of exploiting magnetic field sensing, favours some superior features as fast response, high sensitivity, low cost, small size, robust, and possible wireless and passive measurement. The functional magnetostrictive thin-film materials are favored as the magneto-sensitive interface owing to their large magnetostrictive coefficient, efficient energy conversion, and non-contact actuation.[1] Their magnetomechanical nature produces magnetostrictive strain and ΔE effect sustaining the external magnetic field. The corresponding changes in physical parameters as density, thickness, and Young modulus of the magnetostrictive coating modulate the SAW propagation. Some meaningful results were reported from the SAW magnetic field sensor configurations using magnetostrictive materials as Ga, FeGa, Ni, and FeCo.[2–9] Kodota et al subsequently presented a SAW magnetic field sensor prototype using interdigital transducers (IDTs) made by magnetostrictive Ni on a quartz substrate, and wireless and passive measurement was offered. Obtained magnetic sensitivity was 730Hz/mT.[2,3] Elhosni et al proposed a similar SAW magnetic sensor with a magnetostrictive-piezoelectric layered structure of Ni/ZnO/IDT/$LiNbO_3$.[4,5] Utilizing the magneto-sensitive Galfenol thin film, a SAW magnetic field sensor was developed by Li et al, a maximum change of 0.64% in SAW velocity was calculated theoretically with a 500nm Galfenol thick film.[6] Zhou et al addresses the experimental and theoretical investigations of SAW magnetic sensor structured by $TbCo_2$/FeCo/Y-cut $LiNbO_3$, a maximum velocity shift close to 20% was achieved by choosing a magneto-elastic film thickness and wavelength ratio of 1.[7] In our group, a FeCo thin-film coated SAW device was

[a]E-mail: wangwenwq@mail.ioa.ac.cn

 

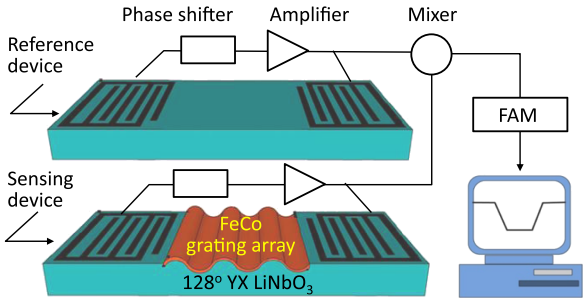


FIG. 1. The scheme of the proposed SAW magnetic field sensor.

proposed for sensing current/magnetic field, obtained sensitivity was up to 8.3KHz/mT based on the theoretical optimization.[9] However, the strong hysteresis effect in magnetostrictive thin-film induces significant hysteresis error, degrading significantly the sensor performance.

In this work, a grating-patterned design is proposed for the FeCo coated SAW magnetic field sensor configuration to suppress the strong hysteresis effect of the magnetostrictive coating. Figure 1 describes the schematic views of the sensor, which consists of differential dual-delay-line oscillators for featuring the temperature compensation, and a FeCo grating array depositing on the SAW propagation path of the sensing device on 128° YX $LNbO_3$ substrate for magnetic field sensing. The magnetostrictive effect in the FeCo stimulated by the magnetic field to be tested modulates the SAW propagation, and the corresponding shift in oscillation frequency was collected to evaluate the measurant. FeCo grating not only weakens the hysteresis effect, but also contributes well to fully release the magnetostrictive strain; hence, high sensitivity, excellent linearity, and low hysteresis error are expected.

## II. THEORETICAL ANALYSIS

First, a theoretical modelization is proposed to investigate the effect from the strip thickness in FeCo grating array on sensor response through an analytical resolution of wave motion equations in layered media of FeCo/$LiNbO_3$.[10] In the simulation, the FeCo coated sensor is simplified as a structure composed of semi-infinite piezoelectric substrate with IDT pattern and a FeCo thin coating, and described in Fig. 2. Acoustic wave propagates along the $x_1$ axis on the $x_1$–$x_2$ plane at $x_3 = 0$. All material parameters of the mediums are transformed into this coordinate system. It is well known that the constitutive wave motion equations in a piezoelectric $LiNbO_3$ are expressed by[11]

$$\begin{cases} \rho_S \dfrac{\partial^2 u^I{}_i}{\partial t^2} - c^{\mathrm{I}}_{ijkl} \dfrac{\partial^2 u^I{}_k}{\partial x_l \partial x_j} - e_{kij} \dfrac{\partial^2 \Phi}{\partial x_k \partial x_j} = 0 \\ e_{jkl} \dfrac{\partial^2 u^I{}_k}{\partial x_l \partial x_j} - \varepsilon_{jk} \dfrac{\partial^2 \Phi}{\partial x_k \partial x_j} = 0 \end{cases}, \tag{1}$$

where Einstein's summation rule is used, and the indices change from 1 to 3. We denote by $u^I$ the mechanical displacements and by $\Phi$ the electric potential. $c^I{}_{ijkl}$, $e_{kij}$, and $\varepsilon_{jk}$ stand for the elastic, piezoelectric and dielectric constants, and $\rho_S$ for the mass density of the piezoelectric substrate, respectively.

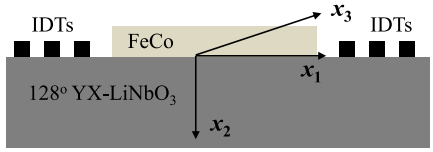


FIG. 2. The coordination system used in the simulation.

Meanwhile, the acoustic wave equation in isotropic and non-piezoelectric FeCo can be written by

$$c^{II}{}_{ijkl}\frac{\partial^2 u^{II}{}_k}{\partial x_l \partial x_j} = \rho_F \frac{\partial^2 u^{II}{}_i}{\partial t^2}, i, j, k, l = 1, 2, 3, \tag{2}$$

here, $c^{II}{}_{ijkl}$ and $\rho_L$ are the stiffness constants and density of FeCo coating.

Owing to the magnetostrictive nature, the FeCo coating produces the magnetostrictive strain, leading to changes in thickness (h) and density ($\rho_L$) of FeCo coating, which are denoted by[12]

$$\begin{cases} h = h_0(1 - \dfrac{\beta}{2}) \\ \rho_L = \rho_0/[(1 + \dfrac{\beta}{2}) \times (1 - \dfrac{\beta}{2}) \times (1 - \dfrac{\beta}{2})] \end{cases}, \tag{3}$$

here, $h_0$ and $\rho_0$ are the thickness and density of unperturbed FeCo coating, respectively, and β denotes the magnetostrictive coefficient of FeCo relating to external magnetic field. Also, the external magnetic field modulates the Young's modulus of the FeCo coating (ΔE effect), which can be measured by using the laser resonance method,[13] and thereout, the corresponding elastic coefficients in FeCo coating are expressed by the perturbed Young's modulus E′ as

$$\begin{cases} c_{11} = \dfrac{E' \times (1 - \mu)}{(1 + \mu)(1 - 2\mu)} \\ c_{12} = \dfrac{E' \times \mu}{(1 + \mu)(1 - 2\mu)} \\ c_{44} = \dfrac{E' \times (1 - 2\mu)}{2(1 + \mu)(1 - 2\mu)} \end{cases}, \tag{4}$$

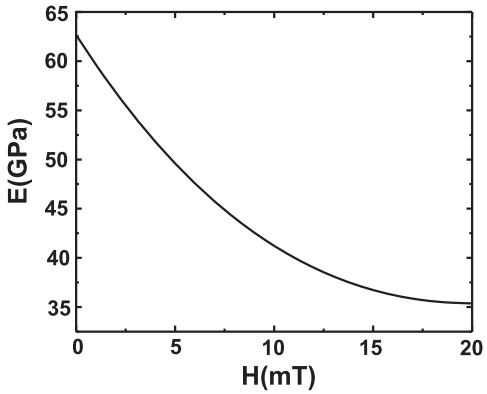


(a)

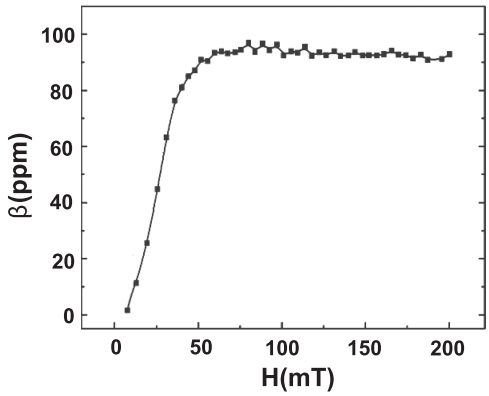


(b)

FIG. 3. The measured correlation among the Young's modulus E (a), and the magnetostrictive coefficient β of FeCo (b), and the magnetic field intensity (H).

TABLE I. The material parameters of $LiNbO_3$ piezoelectric substrate and FeCo film.

| Materials parameters | | Values | |
|---|---|---|---|
| | | $LiNbO_3$ | FeCo |
| Stiffness Coefficients ($10^{11}$N m$^{-2}$) | $C_{11}$ | 2.03 | 0.785 |
| | $C_{12}$ | 0.53 | 0.516 |
| | $C_{13}$ | 0.75 | |
| | $C_{14}$ | 0.09 | |
| | $C_{33}$ | 2.45 | |
| | $C_{44}$ | 0.6 | 0.312 |
| Piezoelectric Modules (C m$^{-2}$) | $e_{31}$ | 0.2 | |
| | $e_{15}$ | 3.7 | |
| | $e_{33}$ | 1.3 | |
| | $e_{22}$ | 2.5 | |
| Permittivity Constants ($10^{-11}$ F m$^{-1}$) | $\varepsilon_{11}$ | 84 | |
| | $\varepsilon_{33}$ | 29 | |
| Density (kg/m$^3$) | | 7450 | 8200 |
| Magnetostrictive constant ($10^{-6}$) | | | 400 |
| Young's modulus (N/m$^2$) | | | 63 |

whereas the Poisson coefficient (μ) of FeCo in Eq. (4) can be considered as a constant (0.3) irrelevant to the magnetic field. Then, exploiting the measured correlation of Young's modulus (E) to magnetic field intensity (H) and the magnetostrictive coefficient (β) to magnetic field intensity (H) pictured in Fig. 3, and mechanical parameters of each medium listed in Table I,[9] the SAW velocity shifts depending on the external magnetic field can be calculated by solving the elastic wave equations (1) and (2) in piezoelectric substrate and FeCo layer using the mechanical and electrical conditions, and allowing determination of the optimal structure parameter.

The sensor response was defined by the difference between the perturbed and unperturbed SAW velocity. Figure 4 displays the influence from the FeCo thickness on sensor response. In the calculation, magnetic field intensity of 20 mT is assumed. Obviously, nonlinear relationship occurs between the sensor response and normalized FeCo thickness, the sensor response increases rapidly with increasing normalized FeCo thickness up to 0.045, and then reaches the maximum value, following which it decrease obviously. This can be explained by taking into account internal binding

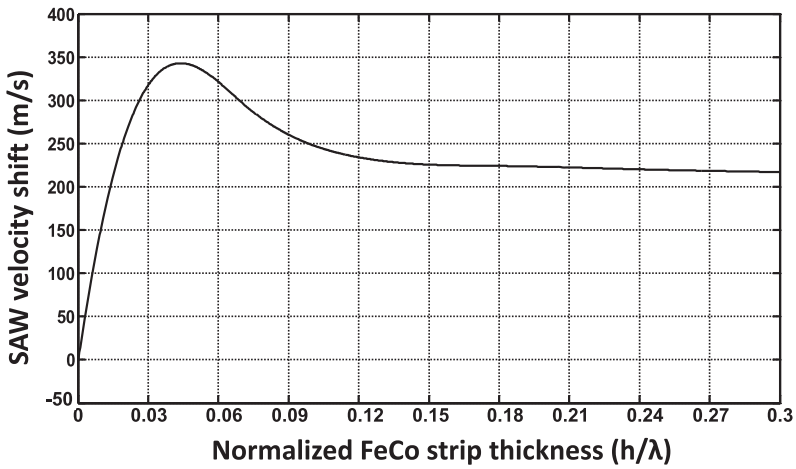


FIG. 4. Calculated SAW velocity shifts depending on FeCo strip thickness, given magnetic field intensity: 20 mT.

force inside the FeCo, which become more significant over the magnetostrictive strain when thicker FeCo coating is applied. Thus, the optimum normalized FeCo thickness is advised to be ~0.045.

## III. TECHNIQUE REALIZATION

The SAW devices for magnetic field sensing is developed by using the overlay photolithographic technique, which is composed of a delay line pattern on 128° YX $LiNbO_3$ substrate with high velocity of 3961 m/s and larger electromechanical factor of 5.5%, and a FeCo grating array deposited along the SAW propagation path between the two photolithographically defined 300nm Al transducers separated by a path length of 2.5mm. Single phase unidirectional transducers (SPUDTs) described in Fig. 5, confining the acoustic energy predominantly in one direction on the piezoelectric substrate surface, were utilized to form the device to reduce the insertion loss.[14] The operation frequency is designed to operate at 300MHz, and corresponding wavelength λ is 13.2μm, and the finger widths in SPUDTs are 3.3 μm (λ/4) and 1.6μm (λ/8), respectively. The fabrication procedure of the sensor chip is depicted below. Aluminium with a thickness of 300 nm was deposited on the cleaned 128° YX $LiNbO_3$ substrate surface using a thermal evaporator. Then, a 1-mm-thick photoresist (PR) was spin-coated, exposed, and developed for the delay line patterns. Aluminium was wet-etched and PR was dissolved in acetone. Next, a 10-mm-thick PR was spin-coated, exposed, and developed again for overlay photolithographic processing for FeCo grating array deposition. The RF magnetron sputtering was utilized for FeCo deposition, and various FeCo grating thickness (200nm, 300nm, 500nm, and 700nm) were achieved via adjusting RF sputtering time. For comparison, the FeCo grating array includes 50 strips with width of 1λ, 3λ and 5λ, and the spacing of the FeCo strips is set to 1λ. The fabricated sensor chips acts as the feedback element in oscillation loop consisting of an amplifier and phase shifter, as depicted in Fig. 1. The differential oscillation frequency signal was

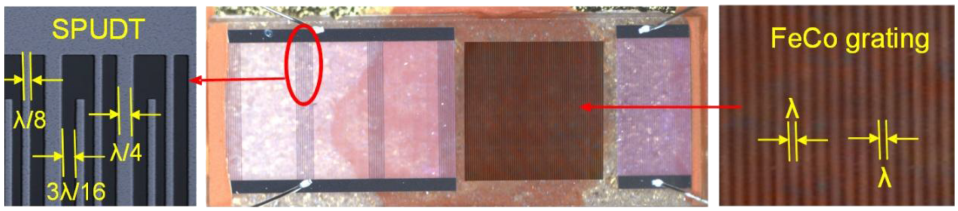


(a)

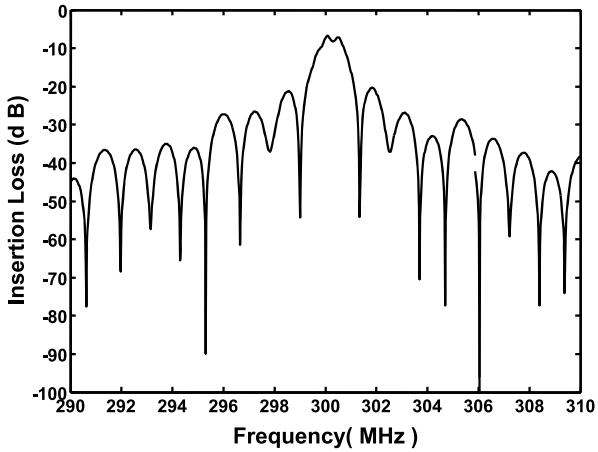


(b)

FIG. 5. (a) Picture and (b) measured frequency characteristic of the fabricated sensor chip with grating-patterned FeCo coating.

picked at speed of 20 point per second by using the frequency acquisition module (FAM) made by the commercial FPGA. For performance comparison, a magnetic field sensor chip coated with 500nm FeCo film was also fabricated. Figure 1 depicted the fabricated sensing device with 1λ width strip and 1λ strip-spacing in grating array. The corresponding frequency characteristic was measured by the network analyzer, as shown in Fig. 5(a). Low insertion loss of ~5dB is benefit for improvement in frequency stability of the differential oscillator.

## IV. RESULTS AND DISCUSSION

### A. Experimental setup

The experimental setup depicted in Fig. 6 for charactering fabricated sensors consists of the fabricated SAW sensor, DC current source, Helmholtz coil for generating the magnetic field, Gauss meter for calibration, and computer terminal for data plotting. The sensor was placed at the central axis of the platform in the middle of the Helmholtz coil system to exposure to strong and uniform magnetic field, and the magnetic field orientation is parallel to the SAW propagation direction ($X_1$ direction in Fig. 2), that is the magnetization direction of the FeCo. The sensor signal is collected at 1 point per 50 ms by the FAM.

### B. Sensor performance evaluation and discussions

First, the effect of the FeCo strip thickness and width in grating array on sensor sensitivity was characterized experimentally at room temperature (25°C) in magnetic field intensities range of

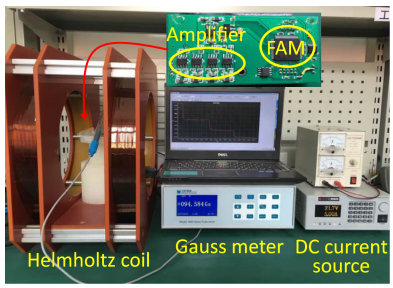


FIG. 6. The experimental setup for characterizing the SAW sensors.

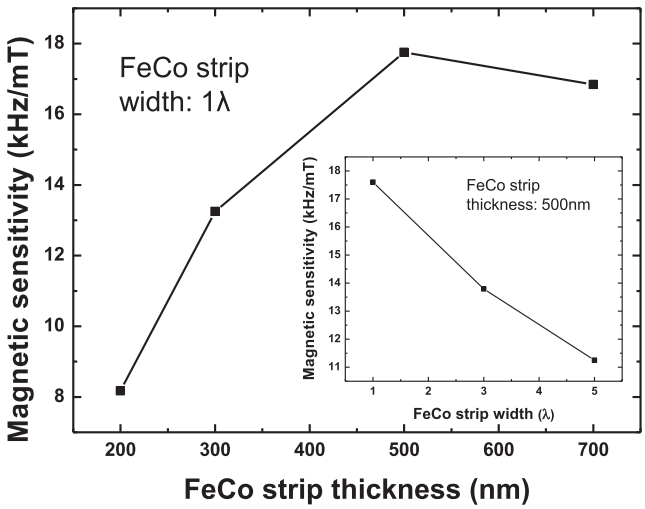


FIG. 7. The measured effect from the FeCo strip thickness and width on magnetic sensitivity.

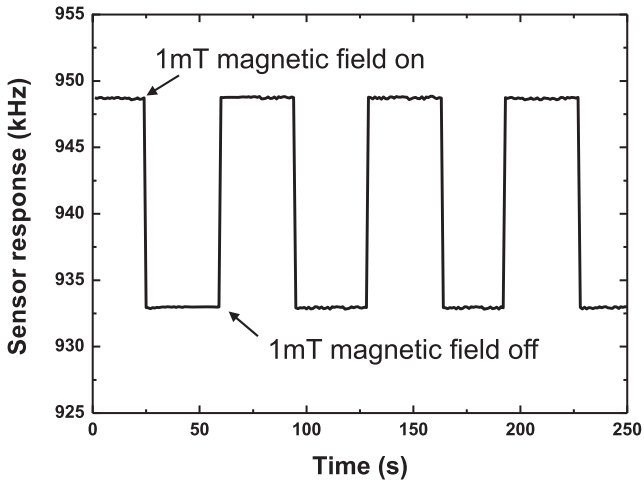


FIG. 8. The repeatability test of the developed sensor.

0~10mT with a 1 mT incremental change. The measured results illustrated in Fig. 7 indicates that sensor sensitivity increases with the FeCo thickness for a thickness up to ~500nm, and slow down afterwards. It means the optimal FeCo thickness was determined as ~500nm (normalized thickness is 0.04), which agrees well with the theoretical predictions described in Fig. 3. Additionally, the sensor sensitivity decreases as the widening in FeCo trip. This phenomenon can be explained by the fully release in the magnetostrictive strain in narrow strip. However, narrower strip is not encouraged because of the poor adhesion and difficult technique. Thereout, FeCo strip thickness of 500nm and width of 1λ are utilized to structure the proposed sensor chip.

Figure 8 shows a typical response profile obtained from three consecutive 35 seconds on-off exposures to magnetic field intensity of 1mT to investigate the repeatability of the fabricated sensor with 500nm FeCo grating array (1λ width strip and 1λ strip-spacing). Three magnetic field exposures are observed in good reproducible run. When magnetic field intensity of 1mT was applied, the sensor response showed a rapid fall to its steady-state value. Furthermore, the sensor response rapidly rises to its initial value after removing the magnetic field intensity. These promising results indicated that excellent repeatability and fast response were obtained from the fabricated sensor.

The continuous response of the stimulated proposed sensor at increasing and decreasing magnetic field intensities was also measured, as shown in Fig. 9. Excellent symmetry is observed in sensor

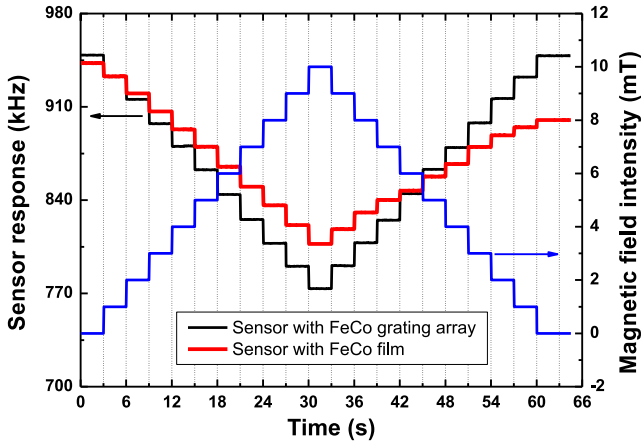


FIG. 9. The continuous response of the stimulated prototype sensor with FeCo grating array at increasing and decreasing magnetic field intensities in comparison with FeCo thin-film coated sensor.

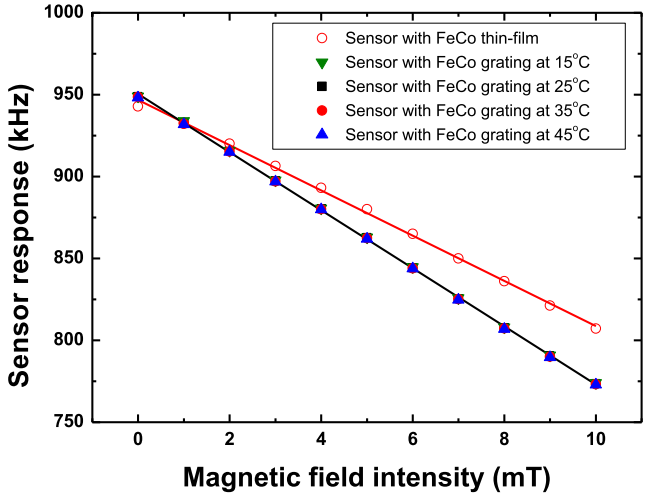


FIG. 10. The sensitivity evaluation of the proposed sensor with FeCo grating array at various temperature, in comparison with the FeCo thin-film coated sensor.

TABLE II. Performance comparison of the sensor with FeCo thin-film and grating array.

| Sensor type | Sensitivity (kHz/mT) | linearity | Hysteresis error |
|---|---|---|---|
| FeCo film coated sensor | 13.8 | 1.61% | 4.721% |
| Grating-patterned FeCo coated sensor | 17.72 | 0.21% | 0.94% |

response at increasing and decreasing magnetic field intensity from the grating-patterned FeCo coated sensor. For comparison, the symmetry testing of the FeCo thin-film coated sensor was also conducted as shown in Fig. 9, the asymmetry phenomenon was obvious because of the larger hysteresis effect in FeCo thin-film over the FeCo grating array. Usually, the hysteresis error was used to evaluated the hysteresis effect, which was defined by $\varepsilon_H=(\Delta y)_{max}/(2y_{RS})\times 100\%$, $(\Delta y)_{max}=\max(y_{ui}-y_{di})$, where $y_{ui}$ and $y_{di}$ are the sensor response at the same current intensity in the process of increasing and decreasing current, $y_{Rs}$ is the full-scale output. From this, a hysteresis error of 0.94% was achieved from the sensor with FeCo grating array, which is far below that in the FeCo film coated sensor (4.72%).

Also, the calibration curves of the sensor response of the developed sensors coated with FeCo grating array and FeCo thin-film were described in Fig. 10. Excellent linearity is observed from the measured magnetic field intensities range. Moreover, evaluated higher sensitivity of 17.6 kHz/mT from the grating-patterned sensor over the FeCo thin-film coated sensor (13.79 kHz/mT) was achieved at temperature of 25°C. Additionally, the crossed temperature effect is compensated well because of the differential oscillator configuration, as shown in Fig. 10. The measured magnetic sensitivity at various temperatures controlled by the temperature chamber were less than 5% (the magnetic sensitivities at temperature of 15°C, 25°C, 35°C, and 45°C are 17.4kHz/mT, 17.6kHz/mT, 17.2kHz/mT, and 17kHz/mT, respectively). This implies that the temperature effect was effectively removed by using the differential oscillation configuration. Table II concludes the measured performance from the SAW sensing device with FeCo grating array and thin-film.

## V. CONCLUSION

In conclusion, a grating-patterned design was conducted for FeCo coated SAW device for sensing magnetic field, the hysteresis effect in FeCo was successfully suppressed. Higher sensitivity, better linearity, and lower hysteresis error were obtained from the sensor prototype with FeCo grating array

over the sensor with FeCo thin-film. From these promising results, we thought that the proposed grating-patterned design on magnetostrictive thin-film is very effective to reduce the hysteresis effect and improve the magnetic sensitivity.

## ACKNOWLEDGMENTS

This work was supported by the National Natural Science Foundation of China (No. 11774381).

[1] S. M. Hanna, IEEE Trans. on Ultrason., Ferroelectr., Freq. Control **34**(2), 191 (1987).
[2] M. Kadota, I. Shigeo, I. Yoshihiro, H. Takuo, and O. Kenjiro, Jpn. J. Appl. Phys. **50**, 07HD07 (2011).
[3] M. Kadota and I. Shigeo, Jpn. J. Appl. Phys. **51**, 07GC21 (2012).
[4] E. Meriem, E. Omar, T. Abdelkrim, A. A. Keltouma, B. Laurent, and S. Frederic, Procedia Engineering **87**, 408 (2014).
[5] E. Meriem, E. Omar, P. W. Sebastien, B. Laurent, and Z. Sergei, Sensors and Actuators A-Physical **240**, 41 (2016).
[6] W. Li, P. Dhagat, and A. Jander, IEEE Trans. on Magnetics **48**, 4100 (2012).
[7] H. Zhou, A. Talbi, N. Tiercelin, and O. B. Matar, Appl. Phys. Lett. **104**, 114101 (2014).
[8] J. Tong, Y. Wang, S. Wang, W. Wang, and Y. Jia, Appl. Sci. **7**, 755 (2017).
[9] W. Wang, Y. Jia, and X. Liu, Smart Mater. Struct. **26**, 025008 (2017).
[10] W. Wang and S. T. He, Sensors and Actuators B-Chem. **138**, 432 (2009).
[11] W. Wang, X. T. Shao, X. L. Liu, J. L. Liu, and S. T. He, Sensors **14**, 3908 (2014).
[12] B. Auld, *Acoustic fields and waves in solids*, vol. 1 (Wiley, New York, 1973).
[13] H. Hong, J. Alloys and Compounds **545**, 182 (2012).
[14] W. Wang, S. T. He, S. Z. Li, M. H. Liu, and Y. Pan, Sensors and Actuators B-Chem. **125**, 422 (2007).